



|  |                                |                    |                               |
|--|--------------------------------|--------------------|-------------------------------|
| <i>Riferimento</i><br>Energy Efficiency NIMMS/SEEIST | <i>DocID</i><br>NIMMS-NOTE-xxx | <i>Rev.</i><br>0.1 | <i>Validità</i><br>2021-02-09 |
|--|--------------------------------|--------------------|-------------------------------|

Proposal

# Power consumption comparison between the room temperature and superconducting version of the NIMMST/SEEIST facility

Abstract

| Autore | Verificato da | Approvato da |
|--------|---------------|--------------|
|        |               |              |

Lista di distribuzione :

## Storico delle Revisioni

| Rev. | Data | Descrizione delle modifiche | Autore/Editore |
|------|------|-----------------------------|----------------|
|------|------|-----------------------------|----------------|



|     |       |             |           |
|-----|-------|-------------|-----------|
| 0.1 | 09-02 | First draft | G.Bisoffi |
|     |       |             |           |
|     |       |             |           |
|     |       |             |           |
|     |       |             |           |
|     |       |             |           |
|     |       |             |           |
|     |       |             |           |
|     |       |             |           |
|     |       |             |           |

**Sommario**

- 1 Introduction ..... 4**
- 2 Specifications of the NIMMS/SEEIST synchrotron-based facility ..... 4**
  - 2.1 Layouts with room-T magnets, magnet specifications ..... 4
  - 2.2 Layouts with SC magnets, magnet specifications..... 6
- 3 Evaluation of the electrical consumption of the CNAO accelerator facilities ..... 8**
  - 3.1 The CNAO hadrontherapy facility ..... 8
  - 3.2 Power consumption estimations, derived from the electrical cabin values ..... 9
  - 3.3 Overall power consumption from the sum of their component contributions..... 11
    - Synchrotron and HEBT*..... 12
    - 3.3.1 *Injector* ..... 14
    - 3.3.2 *Other contributions to be added* ..... 16
    - 3.3.3 *Sum of the consumption from all components* ..... 16
  - 3.4 Power consumption in therapy and non-therapy hours..... 16
    - 3.4.1 *Distribution of energies for 2020* ..... 18
    - 3.4.2 *Use of the various beam lines* ..... 18
- 4 Layout options for the NIMMS/SEEIST facility with room temperature and with superconducting magnet..... 18**
  - 4.1 NC cases. .... 18
  - 4.2 Use of ramped SC magnets for the NIMMS/SEEIST facility. .... 19
  - 4.3 SC Gantry..... 19
    - 4.3.1 *Mikko Karppinen*..... 19
    - 4.3.2 *SC magnets*..... 20
    - 4.3.3 *Rob van Weelderen*..... 21
    - 4.3.4 *Cost of the cryogenic equipment: a comparison* ..... 22



- 4.3.5 Remaining questions.....22
- 4.3.6 NC magnets .....22
- 4.4 SC synchrotron versions.....22
  - 4.4.1 SC magnets .....22
  - 4.4.2 Additional open points for GB.....24
  - 4.4.3 NC magnets .....25
  - 4.4.4 Square-shaped.....25
  - 4.4.5 Triangle-shaped.....25
- 5 Method adopted to estimate power consumption at the NIMMS/SEEIST synchrotron-based facility ..... 25**
  - 5.1.1 Universal model for the energy efficiency comparison .....25
  - 5.1.2 Energy use for therapy treatment .....25
  - 5.1.3 Energy use for therapy tests, machine tests, basic science .....25
- 5.2 Cryogenic efficiency.....26
- 5.3 Overall power consumption of the two SC versions.....26
- 6 Ancillary topics to be addressed. .... 26**
- 7 Added notes, for further possible considerations ..... 27**
  - 7.1 LNL Infrastructure from high to medium voltage lines.....27
  - 7.2 CNAO maximum peak power needed, infrastructure details and electrical contract.....27
  - 7.3 Cost of energy .....28
  - 7.4 Options for layout improvement, impacting on overall efficiency .....28

# 1 Introduction

To be written

*(Scope of SEEIST energy efficient infrastructure, including the accelerator. The comparison between the NC and the SC options being one of the most important items to be assessed in this comparison. All for higher current beam, flash therapy etc.)*

## 2 Specifications of the NIMMS/SEEIST synchrotron-based facility

### 2.1 Layouts with room-T magnets, magnet specifications

The layout of the two room temperature options for the facility are shown in fig. 1 and (options RT1 and RT2 in the text). RT1 is an advanced synchrotron featuring, versus present generation machines, a higher beam intensity for faster treatment ( $2 \times 10^{10}$ , 20 times higher), multiple energy extraction (multiple flat-tops), an additional fast extraction for FLASH operation. Moreover, the injector will be redesigned at a higher frequency, to reduce its cost and allow parallel isotope production. Acceleration of p, He, C, O, Ar beams from three ion sources is foreseen.

Data related to RT1 are shown in table 1. While the energy at injection will be identical or similar to that at operational machines (HIT, CNAO, MedAustron), the maximum extraction energy for heavier beams (e.g.  $^{12}\text{C}^{6+}$ ,  $^{16}\text{O}^{8+}$ ) will reach 430 MeV/u, with a maximum rigidity in the synchrotron dipoles of 6,62 Tm, corresponding to a maximum operational field of 1,5 T. The synchrotron magnet ramp rate is 2,26 T/s. The High Energy Beam Transport lines (HEBT) may deliver the beam to three treatment rooms, in one case from the horizontal direction, in another from both horizontal and vertical directions, in a third case with a superconducting gantry.

*As to the power consumption: Number of dipoles, quads-families and gradient at maximum energy, sextupoles, cavity, septa, other elements. Prepare a table here.*

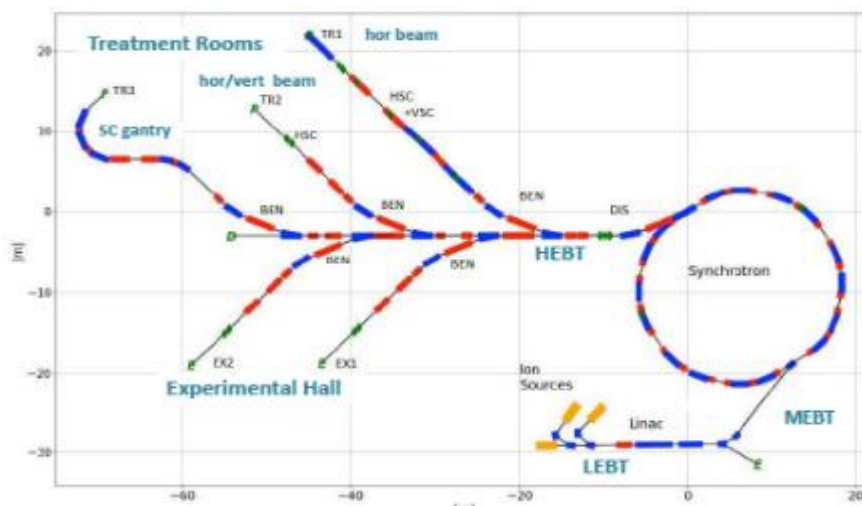


Fig.1 Layout of the advance synchrotron (RT1)

| Injection/Acceleration   | Unit  | p                     | $^4\text{He}^{2+}$  | $^{12}\text{C}^{6+}$ | $^{16}\text{O}^{8+}$ | $^{36}\text{Ar}^{16+}$ |
|--|-------|-----------------------|---------------------|----------------------|----------------------|------------------------|
| Particle after stripping   |       | <b>p</b>              | $^4\text{He}^{2+}$  | $^{12}\text{C}^{6+}$ | $^{16}\text{O}^{8+}$ | $^{36}\text{Ar}^{16+}$ |
| Energy   | MeV/u | 7                     |                     |                      |                      |                        |
| Magnetic rigidity at injection   | Tm    | 0.38                  | 0.76                | 0.76                 | 0.76                 | 0.86                   |
| Extraction energy range (**)   | MeV/u | 60 – 250<br>(1000)    | 60 – 250<br>(430)   | 100 - 430            | 100 - 430            | 200 – 350              |
| Magnetic rigidity at highest energy (for therapy)                                | Tm    | 2.42                  | 4.85                | 6.62                 | 6.62                 | 6.62                   |
| Maximum nominal field  | T     | 1.5                   |                     |                      |                      |                        |
| Maximum number of particles per cycle  |       | $2.6 \cdot 10^{11}$   | $8.2 \cdot 10^{10}$ | $2 \cdot 10^{10}$    | $1.4 \cdot 10^{10}$  | $5 \cdot 10^9$         |
| Ramp-up rate   | Tm/s  | <10                   |                     |                      |                      |                        |
| Ramp-down time of magnets  | s     | 1                     |                     |                      |                      |                        |
| Spill ripple, intensity ratio $I_{\text{max}}/I_{\text{mean}}$ (average on 1 ms) |       | < 1.5                 |                     |                      |                      |                        |
| Slow extraction spill duration with multi-energy                                 | s     | 0.1 – 60              |                     |                      |                      |                        |
| Fast extraction  | s     | < $0.3 \cdot 10^{-6}$ |                     |                      |                      |                        |

Table 1 – Specification of the NIMMS/SEEIST synchrotron in its standard room-T version

An alternative room temperature design (RT2) has been conceived, which is sketched in fig.2. It is based on Double Bend Achromat cells, with dispersion-free drift sections and only 12 dipoles and 14 quadrupoles [X. Zhang, U. Melbourne]. **Does a parameter table exist? As to the power consumption: Number of dipoles, quads-families and gradient at maximum energy, sextuples, cavity, septa, other elements**

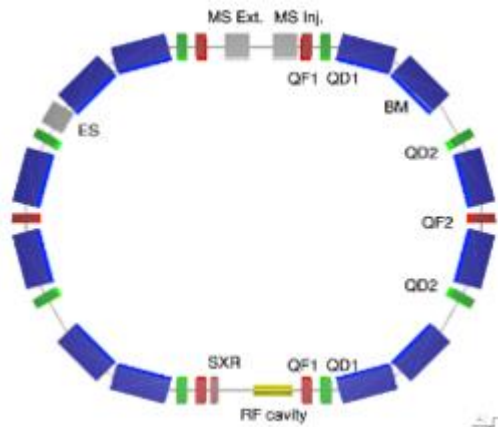


Fig.2 – Scheme of the room temperature synchrotron based on DBA cells.

The injection MEBT and the extraction line of RT1 will differ slightly from RT2, due to the different shape and size of the synchrotron. However, before an overall scheme is studied the same injector and HEBT systems will be assumed when comparing these two solutions in terms of energy consumption.

The gantry proposed for both RT1 and RT2 is superconducting. For the sake of comparison, however, the gain in energy efficiency versus a room temperature gantry with equivalent beam features will be analysed in par. 4.1.

**2.2 Layouts with SC magnets, magnet specifications**

The main advantage of SC magnets for synchrotron and gantry, beyond energy efficiency, is the reduction of the footprint of the accelerator. To take this advantage to an extreme of compactness, solutions with just one or two beamlines have been proposed in this case (gantry, gantry plus a horizontal line), since the footprint of treatment areas and HEBTs are a significant fraction of the total. However, for the sake of a fair comparison, all three HEBT configurations of fig. 1, 3 and 4 will be analysed so that all combinations of synchrotrons and beam lines can be calculated.

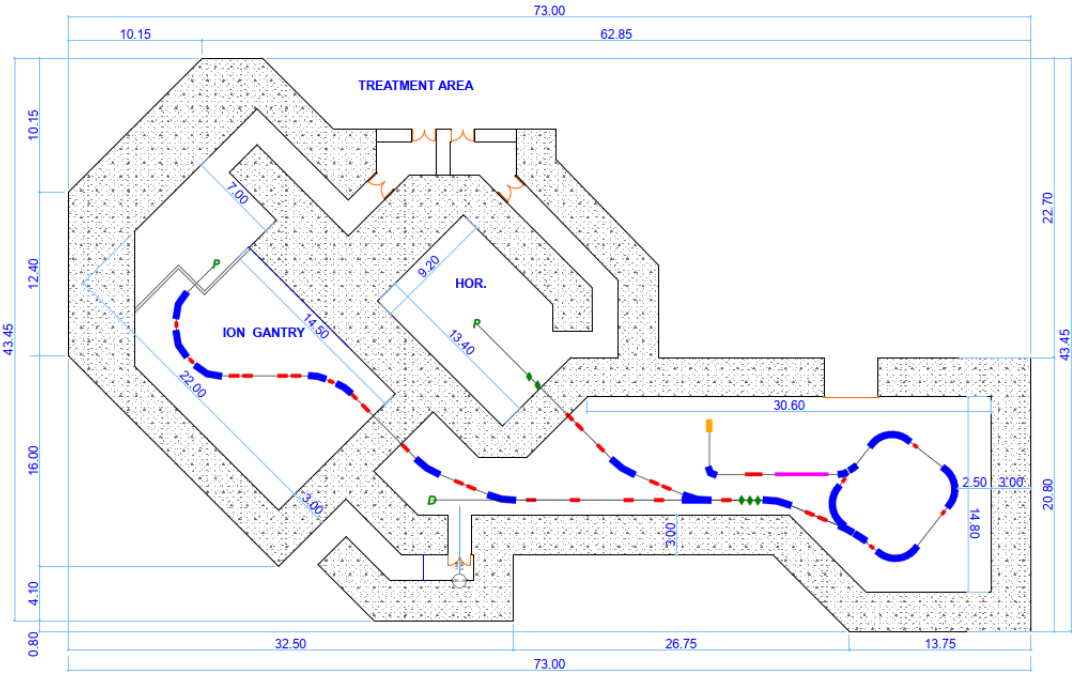


Fig.3 Layout of a compact square-shape synchrotron with SC magnets and two treatment rooms

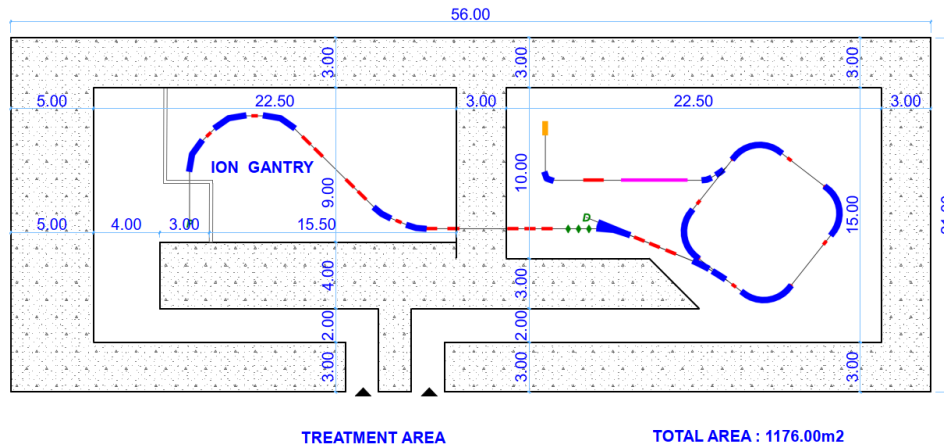


Fig.4 Layout of a compact square-shape synchrotron facility, with SC magnets and one treatment room

Table 2 shows the main parameters of the square-shaped superconducting synchrotron, where a maximum bending field of 3,5 T is assumed.

|                               |                 |
|-------------------------------|-----------------|
| Circumference                 | 27 m            |
| Injection energy              | 7 MeV/u         |
| Extraction energy             | 100 → 430 MeV/u |
| Straight section 1            | 3 m             |
| Straight section 2            | 3.6 m           |
| AG-CCT Max. bending field     | 3.5 T           |
| AG-CCT Bending radius         | 1.89 m          |
| AG-CCT Magnetic bending angle | 90°             |

Table 2 Main parameters of the square-shaped superconducting synchrotron

As an alternative to the square-shape superconducting synchrotron, a triangle-shape one has been considered too and its lattice parameters preliminarily investigated. The latter will be further gain in compactness, while the number of straight sections is sufficient for the injection, extraction and acceleration functions. Fig.5 shows the schemes of these two superconducting synchrotron options

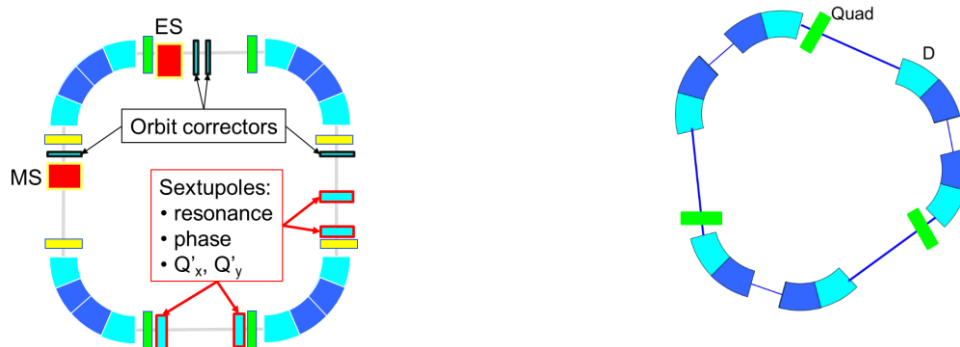


Fig.5 – Scheme of the square-shape and triangle-shape synchrotrons



| Riferimento                    | DocID          | Rev. | Validità   |
|--------------------------------|----------------|------|------------|
| Energy Efficiency NIMMS/SEEIST | NIMMS-NOTE-xxx | 0.1  | 2021-02-09 |

As to the SC synchrotron options, table 3 shows the number and design features of both the SC and room-T magnets involved, for the purpose of their power consumption evaluation.

(to be prepared with EB)

#### Table 4

It must be pointed out that a substantial challenge in the SC magnet design and construction is the maximum achievable field ramp, which will be discussed in par.4.3 and is assumed to be 1 T/m.

### 3 Evaluation of the electrical consumption of the CNAO accelerator facilities

In this study, the electrical consumption – averaged over a whole year of operation – of the hadrontherapy facility CNAO has been investigated. In the limits in precision of this analysis (examined in more depth in the following), the experimental data of CNAO serve as a benchmark for studying the power consumption of the various configurations of the NIMMS-SEEIST facility.

After a description of the CNAO facility (par. 3.1), power consumption data are given, as obtained by values obtained at the main electrical cabin (par 3.2) and by the computed individual contributions of the more power-consuming machine sections (par. 3.3).

#### 3.1 The CNAO hadrontherapy facility

The goal of this study is to estimate the power consumption of the CNAO synchrotron both as a whole and as macro components.

The layout of the CNAO facility is shown in fig.6. A synchrotron with 16 dipole magnets and 24 quadrupoles, split in 3 independent families, receives either a proton (p) or carbon (C) beam from two ECR ion sources and one 7 MeV/u injector. The High Energy Transport Line (HEBT) can deliver the accelerated beam to one of the three treatment rooms (TR), one equipped with horizontal and vertical beam lines, the other two with only a horizontal beam line.

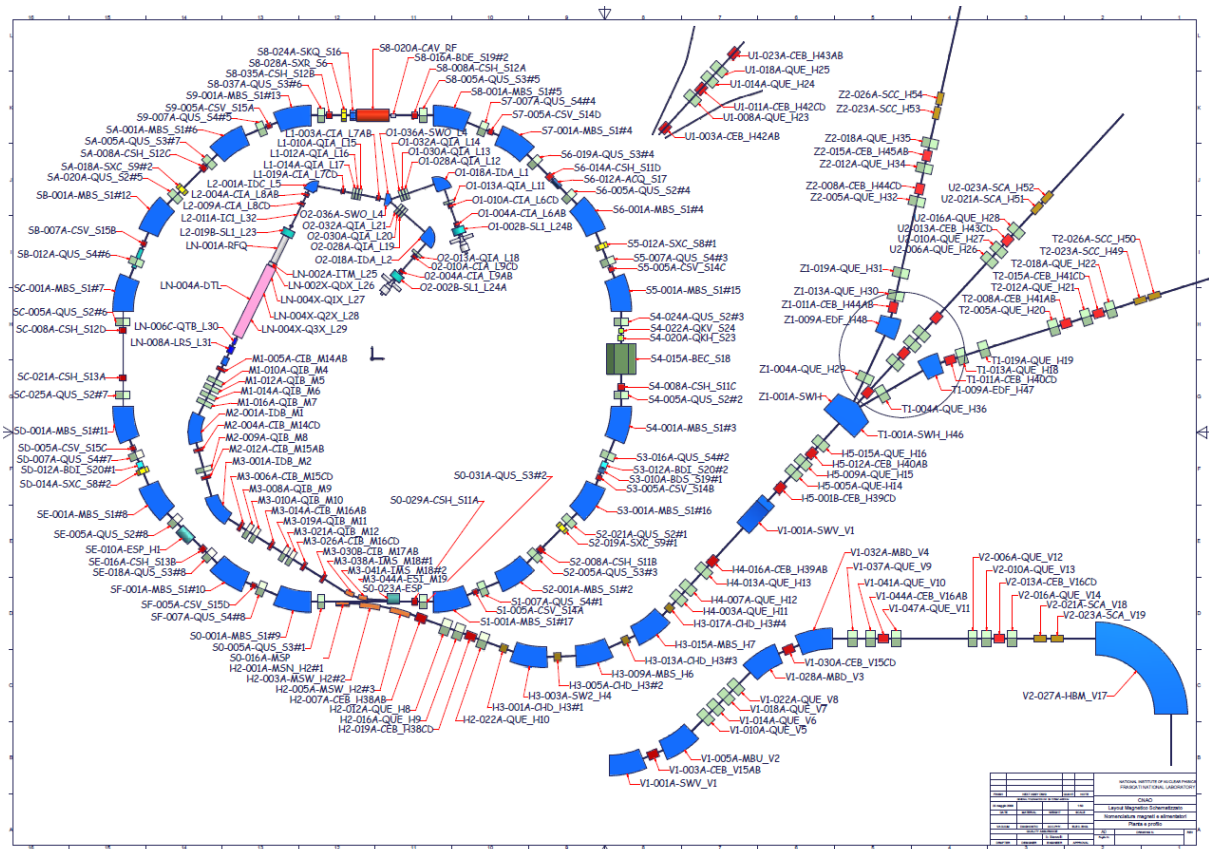
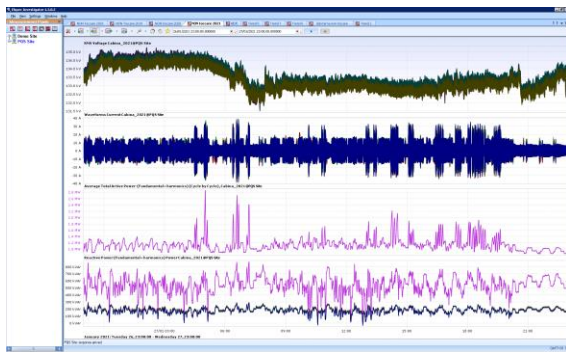


Fig.6 – Layout of the CNAO hadrontherapy facility. The synchrotron feeds three treatment rooms (TRs): the two lateral rooms (#1 and 3) receive an horizontal beam while the central room (#2) receives both an horizontal and a vertical beam.

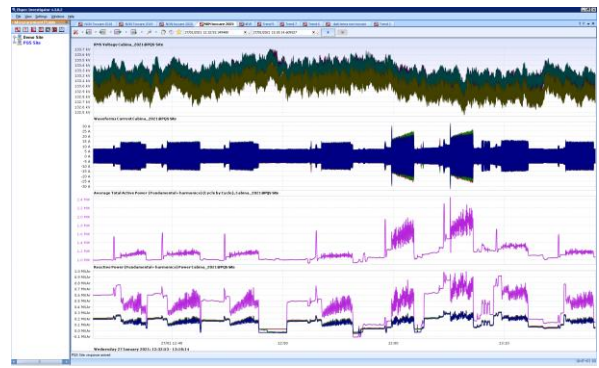
**3.2 Power consumption estimations, derived from the electrical cabin values**

The goal of this benchmarking study is to estimate the power consumption of the CNAO synchrotron both as a whole and as the sum of its macro components.

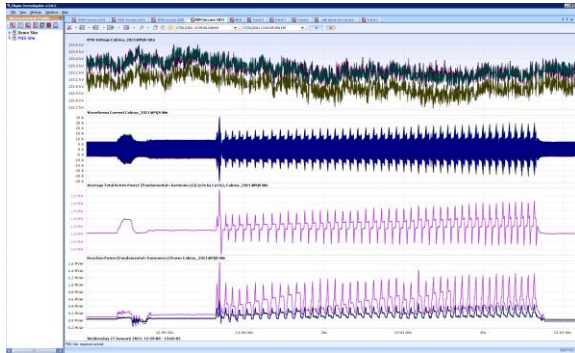
The starting point is that unfortunately no direct log/measurement of the power required by the whole machine itself or its parts is available. CNAO has an electrical/energy monitor unit installed on the high voltage feeder that comes from the national distribution grid (132 kV). The monitor stores in a database voltage and current waveforms for each grid cycle (256 samples per cycle). These waveforms can be used to compute power, energy, total harmonic distortion (THD), RMS values and so on. Some examples of what this system logs are given in fig.7. In each graph the RMS voltage, the current waveform, active and reactive power are shown, for various time spans in typical days (see figure caption for more details). A steady state consumption of around 1 MW is due to the 100% d.c. elements of the accelerator, the auxiliary plants, utilities of buildings and offices.



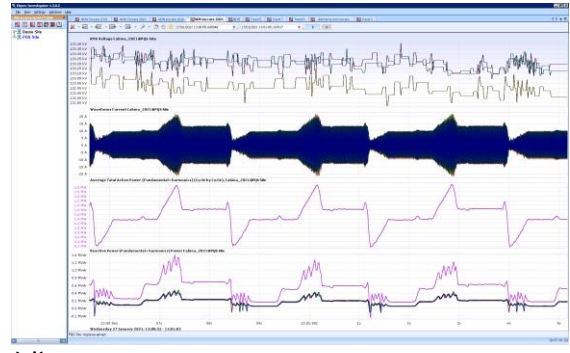
(a)



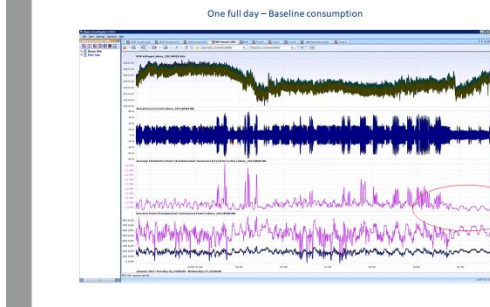
(b)



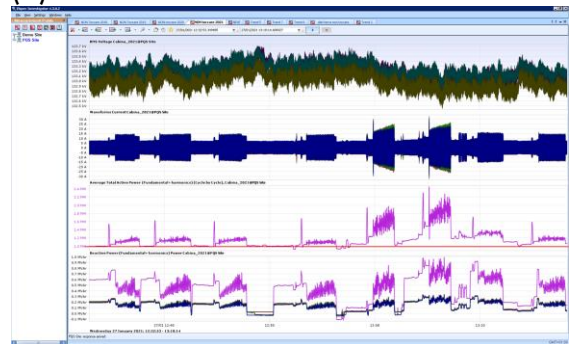
(c)



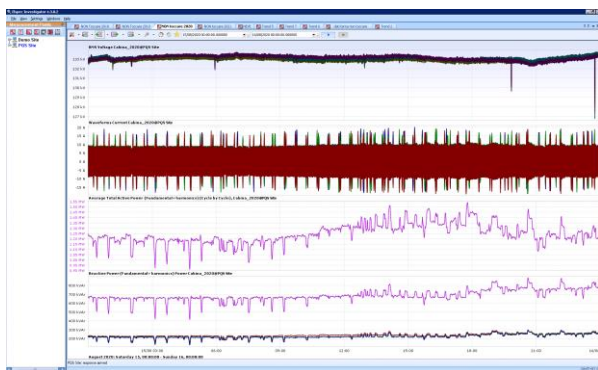
(d)



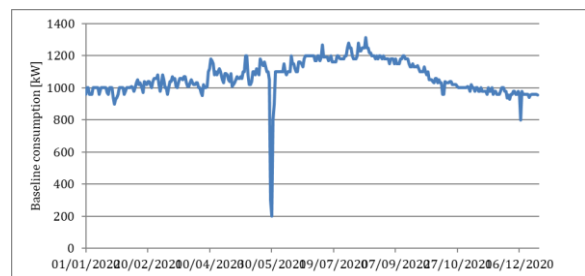
(e)



(f)



(g)



(h)

Fig.7 – Examples of system logs at the main electrical cabin at CNAO. Plot (a) spans 24 hours of a sample working day (24 hours); plot (b) is a 50 minute zoom where treatment cycles of increasing energy with p and C (the latter characterized by a higher power consumption) can be seen; plot (c), over 3 minutes, shows a single C treatment fraction, and its individual ramps can be seen in plot (d), over 8 s, in greater detail. Plots (e) and (f) are the same as plots (a) and

(b), where the baseline consumption of around 1 MW, with idle machine at night times, is highlighted in the red ellipse and by the red line, respectively. Plot (g) shows the daily consumption on Aug 15, 2020, a holiday where the machine was off and the standard infrastructures were on, showing that on summer days HVAC consumption raises the steady state consumption from around 1 MW to 1,2 MW at night time and 1,35 MW at day time. This behaviour can be better seen in plot (h), where the baseline consumption over a whole year is shown, with the big drop in May 2020 due to a periodical maintenance on CNAO substation and a small drop in December, due to an accident on the town grid.

The baseline consumption of fig.7 is due to the building infrastructures (e.g. lightning, HVAC), the plants (e.g. pumping stations, transformers) and the DC part of the accelerator (e.g. the injector, the vacuum pumps). Its average over year 2020 is 1,066 kW, corresponding to  $9,338 \times 10^6$  kWh. CNAO's consumption, as obtained by the electricity bills, is about  $11,7 \times 10^6$  kWh in 2020, which implies that the time-variable part of the electrical consumption is about 2,360,000 kWh, with an average power of 270 kW. This value does not correspond to the overall average power consumption of the accelerator because, as specified above, only some parts of the synchrotron do consume power exclusively when acceleration takes place. The quasi-DC components (e.g. injector, pumping stations, power converters when in idle state, etc.) are accounted for in the baseline consumption and cannot be separated from the consumption of non-accelerator components.

Some sources of consumptions, belonging in principle to the baseline quasi-DC consumption, are indeed acceleration correlated and can be computed with reasonable accuracy. A major one is the power consumption of the chiller, treating the cooling water of both magnets and power converters, activated as a reaction to the increase of the machine water temperature.

It may be noted, incidentally, that the peak power consumption of the facility, during magnet ramps, may achieve a maximum of around 7 MW.

### 3.3 Overall power consumption from the sum of their component contributions

Once concluded that time-variable components, as seen from the electrical cabin, have a yearly average power consumption of 270 kW and that the DC part of the facility consumption is embedded in the overall DC consumption of the CNAO center, a complementary approach has been taken, in trying to estimate, individually, the contribution of the main accelerator systems.

Log files exist for each machine cycle that produces an accelerated beam, which includes information about: the accelerated particle, the cycle duration and the treatment room (TR) that was used, which defines the setup of the extraction lines. The use of the vertical line is particularly relevant, because of the large consumption contribution of the big  $90^\circ$  dipole.

Each patient's treatment or in general each beam activity is made of a sequence of cycles. The ring magnets (dipoles, quadrupoles and sextupoles) follow a variable current reference with a given shape for each cycle (fig.8). The value of the flat-top changes with energy.

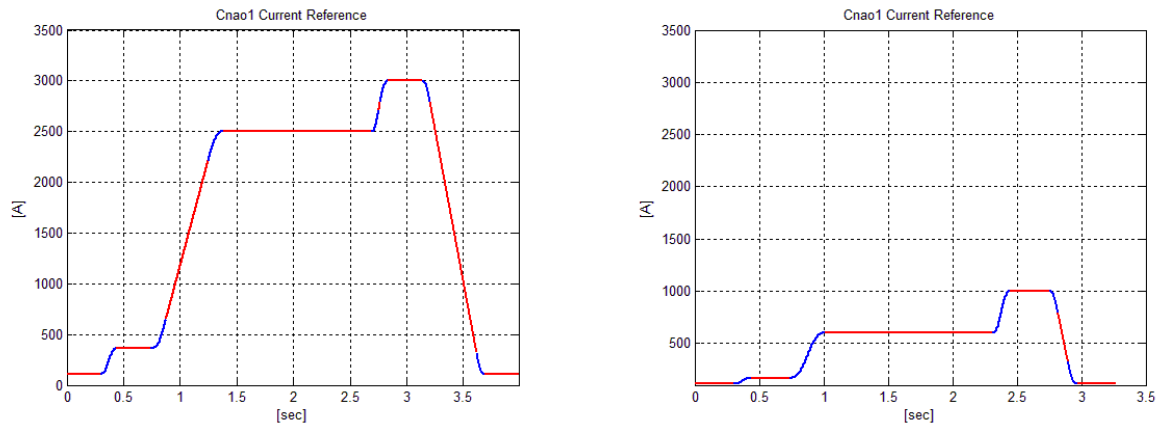


Fig.8 - Ring dipoles current reference: carbon beam (left),

The extraction lines work instead in “quasi DC” mode: they go to an initial setpoint at the beginning of the treatment and keep it until the energy of the extracted beam changes (so they do not ramp cyclically as synchrotron magnets do).

For a certain TR only the magnets required to bring the beam in that TR are supplied.

As mentioned in par.3.2.2., the injector is kept always on, at the conditions of the latest beam used (p or C), and therefore it is considered as a DC contributor to energy consumption.

In addition, when no acceleration is taking place, all the power supplies of the ring and of the extraction lines are on: **around 0,5 kW per power supply which, with ~90 power supplies, delivers a 45kW additional contribution for the 75,6% of the time of the idle state, i.e. 34kW average.**

### Synchrotron and HEBT

For most power converters of synchrotron and HEBT lines, the exact value of the flat top electrical current, or of the DC reference corresponding to each cycle code, was extracted from the repository.

By a large extent, the most power consuming elements in the synchrotron are the dipoles. The exact current shape vs. time function of the ring dipoles can be calculated starting from the flat top value and the time settings of the machine cycle (which are registered values). Then the exact power consumption can be calculated for each combination of flat top value and cycle duration.

The big 90° dipole of the vertical beam line has a significant power consumption (790kW, i.e. 1050kW including the power supply efficiency), when in use at its maximum current.

The following items were considered:

- Ring dipoles (16+1 in series; one converter)
- Ring quadrupoles (three families of 8 quads each) and sextupoles (two families of 2 magnets each). These have been approximated to DC machines working at a setpoint equal to the flat top (*overestimation of power consumption*).
- Resonance sextupole (1 magnet, approximated to a DC machine working at a setpoint equal to the flat top, *overestimation of power consumption*)
- Magnetic septum at injection (two setpoints, one for P and one for C; active only when acceleration takes place)



- Magnetic septum at extraction
- Dipoles of the extraction lines (minimum of 3, exact number depends on the TR)
- 90° dipole (active for the vertical line only)

The calculation takes into account the efficiency of each power converter, an experimental datum reported, however, at the maximum current of the respective converter (*underestimation of average power consumption*).

The following items were neglected:

- Quadrupoles of the extraction lines, difficult to estimate, since each one has a different setpoint for each energy (*underestimation of power consumption*)
- Scanning magnets.

The overall outcome of this analysis is shown in table 3 in which, for each month of 2020, the total “on-time” of the facility is reported (in seconds), the average power consumption of all above mentioned elements and that of the dipoles only.

The average use (on-time) of the facility is 641000 s, corresponding to 7,41 days/month, the average power consumption of these elements is 130,6 kW, out of which the average consumption of the 16+1 dipoles is 44,5 kW.

| <u>Month</u> | <u>Activity [s]</u> | <u>Power consumption [W]</u> | <u>Dipoles power consumption [W]</u> |
|--------------|---------------------|------------------------------|--------------------------------------|
| January      | 577,648.0           | 131,353.3                    | 41,305.1                             |
| February     | 668,246.0           | 156,492.0                    | 51,197.8                             |
| March        | 688,599.0           | 132,702.1                    | 43,923.3                             |
| April        | 649,965.0           | 114,887.2                    | 37,928.4                             |
| May          | 631,827.0           | 124,176.6                    | 43,323.9                             |
| June         | 720,644.0           | 155,020.9                    | 57,111.9                             |
| July         | 662,333.0           | 130,723.3                    | 46,751.7                             |
| August       | 580,451.0           | 132,746.2                    | 47,656.8                             |
| September    | 552,052.0           | 113,130.7                    | 38,141.3                             |
| October      | 601,033.0           | 102,745.3                    | 34,472.3                             |
| November     | 709,333.0           | 146,565.4                    | 49,559.6                             |
| December     | 650,387.0           | 127,227.3                    | 43,130.8                             |

Table 3 – For each month of 2020, the overall use of the facility (on-time) is given, together with the average power consumption of the most relevant elements of synchrotron and beam lines, out of which the average power consumption of the synchrotron dipoles is singled out.

Despite the COVID-19 pandemic, year 2020 represents rather well the yearly power consumption of CNAO. This can be seen in fig.7, where monthly use of the facility, synchrotron+HEBT and dipole power consumptions are reported for 2018, 2019 and 2020.

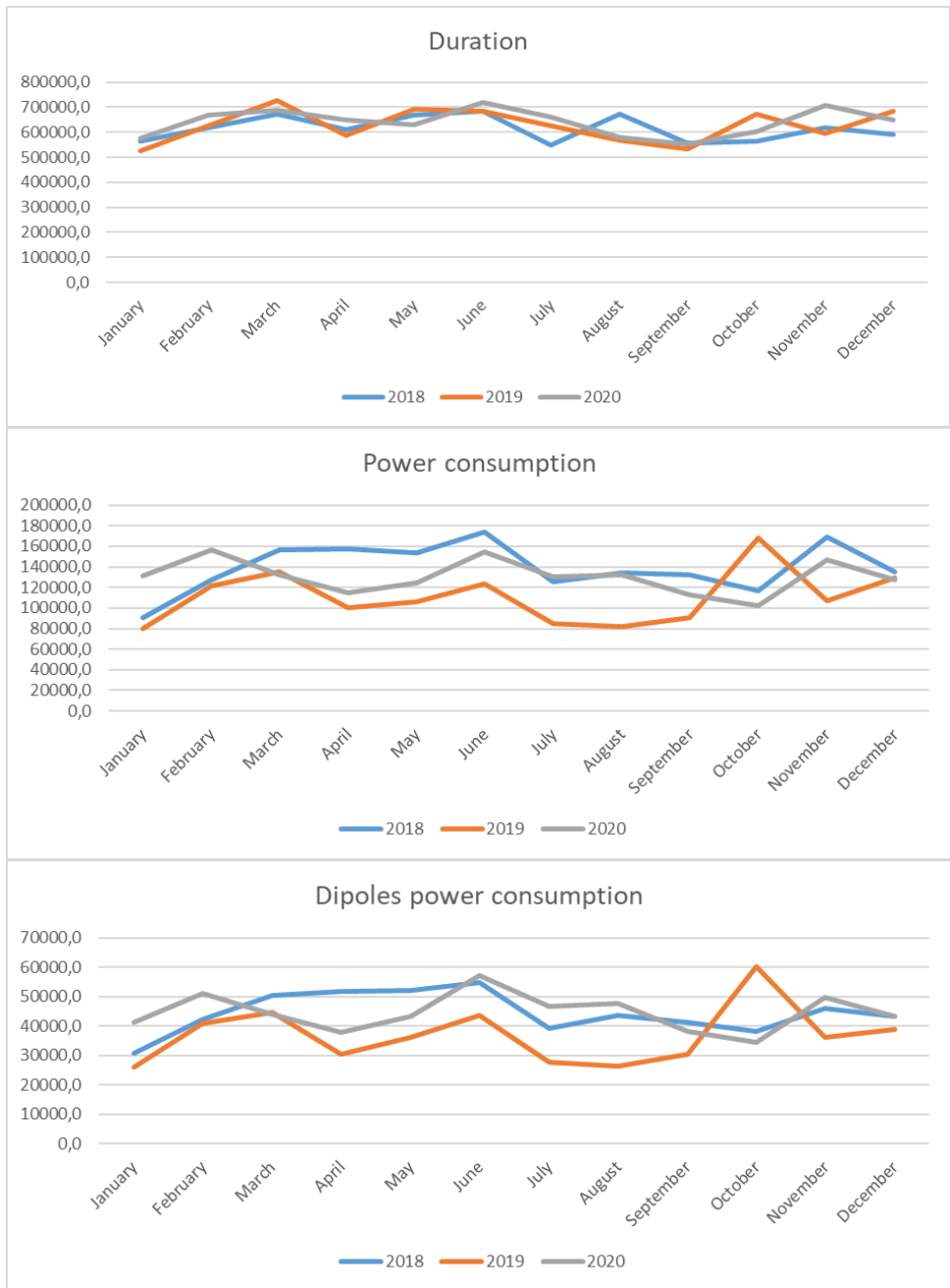


Fig.7 – Duration of use of the facility (in s), power dissipation of the main synchrotron+HEBT elements and of the synchrotron dipoles alone in years 2018-2019-2020. It shows that 2020 can be considered a rather “typical” year.

### 3.3.1 Injector

In the following, “injector” is defined as the portion of the facility from the ion sources to the electrostatic septum injecting the beam into the synchrotron, whereas “linac” is referred to the accelerating part of the injector, i.e. the RFQ and the IH-DTL. The injector (LEBT + LINAC + MEBT) works in DC: the setpoint changes only when the particle (p or C) is changed.

The LINAC cavities (RFQ and IH-DTL) work in pulsed mode, but they are constantly pulsed at 10 Hz, a higher rate than needed for acceleration, so as to keep the cavities at thermal equilibrium. The effective RF duty cycle is 0.5%, with only one pulse per machine cycle used to



accelerate the beam; the duration of the machine cycle can vary between 1 and 17 seconds.. The linac quadrupoles are not included in the power consumption estimation: given their effective duty cycle (on only with beam pulses, not with “thermal” cycles, is negligible.

Additionally, the LINAC RF amplifiers have a fixed consumption due to the filaments of the tetrodes, which ends up being a non-negligible fraction of their total consumption.

The various parts of the injector have been analysed: the sources and the two Low Energy Beam Transport lines (LEBT) before their merging (p and C beam lines contributions must be summed, as they are always on); the common part of the LEBT (with different values for their fixed setting for p and for C beams); the linac (also split between p and C). The result is shown in table 4.

**Particle dependent LEBT part**

**Protons**

| Name         | Type | Setpoint[A] | Power [W]     |
|--------------|------|-------------|---------------|
| L1           | Dip  | 43.8        | 582.0         |
| L11          | Quad | 9.0         | 5.4           |
| L6A          | Corr | -25.5       | 398.3         |
| L6B          | Corr | -10.0       | 61.4          |
| L6C          | Corr | 41.2        | 1044.9        |
| L6D          | Corr | -1.1        | 0.8           |
| L12          | Quad | 54.0        | 195.4         |
| L13          | Quad | 118.0       | 934.2         |
| L14          | Quad | 68.0        | 310.2         |
| <b>Total</b> |      |             | <b>3532.7</b> |

**Carbon**

| Name         | Type | Setpoint[A] | Power [W]     |
|--------------|------|-------------|---------------|
| L2           | Dip  | 43.7        | 579.9         |
| L18          | Quad | 14.0        | 13.1          |
| L9A          | Corr | 19.4        | 231.2         |
| L9B          | Corr | 0.1         | 0.0           |
| L9C          | Corr | 0.1         | 0.0           |
| L9D          | Corr | 9.0         | 49.8          |
| L19          | Quad | 41.5        | 115.5         |
| L20          | Quad | 95.5        | 611.8         |
| L21          | Quad | 62.9        | 265.7         |
| <b>Total</b> |      |             | <b>1866.9</b> |

**Grand total: 5399.6**

**Common part of the LEBT + MEBT**

**Protons**

| Name         | Type | Setpoint[A] | Power [W]     |
|--------------|------|-------------|---------------|
| L4           | Quad | -16.2       | 75.6          |
| L5           | Dip  | 146.2       | 1237.0        |
| L7A          | Corr | 25.7        | 407.2         |
| L7B          | Corr | 0.0         | 0.0           |
| L7C          | Corr | 0.0         | 0.0           |
| L7D          | Corr | 9.0         | 49.7          |
| L8A          | Corr | 10.8        | 71.9          |
| L8B          | Corr | -10.8       | 71.6          |
| L8C          | Corr | -24.7       | 375.5         |
| L8D          | Corr | 21.2        | 275.1         |
| L15          | Corr | 70.0        | 328.9         |
| L16          | Corr | 129.0       | 1116.4        |
| L17          | Corr | 65.0        | 283.4         |
| M1           | Dip  | 125.5       | 1803.6        |
| M2           | Dip  | 125.9       | 1815.4        |
| M4           | Quad | 76.3        | 727.9         |
| M5           | Quad | 0.5         | 0.0           |
| M6           | Quad | 60.2        | 453.0         |
| M7           | Quad | 46.5        | 270.3         |
| M8           | Quad | 25.0        | 78.1          |
| M9           | Quad | 22.0        | 60.5          |
| M10          | Quad | 21.5        | 57.8          |
| M11          | Quad | 13.0        | 21.1          |
| M12          | Quad | 6.0         | 4.5           |
| M16A         | Corr | -0.2        | 0.0           |
| M16B         | Corr | 2.5         | 2.7           |
| M16C         | Corr | 1.0         | 0.4           |
| M16D         | Corr | 6.5         | 18.5          |
| M17A         | Corr | 4.8         | 10.1          |
| M17B         | Corr | -4.8        | 10.1          |
| <b>Total</b> |      |             | <b>9626.1</b> |

**Carbon**

| Name         | Type | Setpoint[A] | Power [W]      |
|--------------|------|-------------|----------------|
| L4           | Quad | 16.8        | 81.8           |
| L5           | Dip  | 144.0       | 1200.5         |
| L7A          | Corr | 18.0        | 199.3          |
| L7B          | Corr | 0.1         | 0.0            |
| L7C          | Corr | -13.0       | 103.6          |
| L7D          | Corr | -6.0        | 22.0           |
| L8A          | Corr | 20.5        | 258.2          |
| L8B          | Corr | 14.3        | 125.1          |
| L8C          | Corr | -5.2        | 16.5           |
| L8D          | Corr | 10.0        | 61.9           |
| L15          | Corr | 60.0        | 241.5          |
| L16          | Corr | 88.0        | 519.3          |
| L17          | Corr | 31.0        | 64.6           |
| M1           | Dip  | 250.1       | 7160.9         |
| M2           | Dip  | 251.1       | 7218.3         |
| M4           | Quad | 149.0       | 2774.8         |
| M5           | Quad | 0.5         | 0.0            |
| M6           | Quad | 120.0       | 1799.4         |
| M7           | Quad | 92.9        | 1078.8         |
| M8           | Quad | 51.0        | 325.1          |
| M9           | Quad | 46.5        | 270.3          |
| M10          | Quad | 45.3        | 256.1          |
| M11          | Quad | 16.1        | 32.4           |
| M12          | Quad | 2.5         | 0.8            |
| M16A         | Corr | 0.0         | 0.0            |
| M16B         | Corr | 6.5         | 18.5           |
| M16C         | Corr | 6.5         | 18.5           |
| M16D         | Corr | 0.0         | 0.0            |
| M17A         | Corr | 5.0         | 10.9           |
| M17B         | Corr | -3.0        | 3.9            |
| <b>Total</b> |      |             | <b>23862.8</b> |

**Grand total: 16744.5**



|                   | Power [W] | Note                        |
|-------------------|-----------|-----------------------------|
| Solenoid Protons: | 2,156     | Fixed setpoint              |
| Solenoid Carbon:  | 1,700     | Fixed setpoint              |
| Solenoids common: | 6,520     | Particle dependent setpoint |

**RFQ**

|           |       |
|-----------|-------|
| Filament: | 3,500 |
| RF        | 1,100 |

**IH-DTL**

|           |        |
|-----------|--------|
| Filaments | 17,400 |
| RF        | 9,500  |

**Total**                                 **41,876**

Table 4 – average power consumption of the main injector parts, where: the particle dependent sections must be summed; for the common part of the LEBT, p or C values can be taken. For the RFQ and the IH-DTL the average power consumption is taken, and similarly for the solenoids (for the one in common, it is assumed that it is set at 50-50 of the time between p and C).

### 3.3.2 Other contributions to be added

- Estimation by Elena/Davide T. on the scanning magnets
- Contribution of power converters and RF amplifiers in idle state for the remaining fraction of the year time.
- Evaluate the balance of over-and-under estimations above
- Fully DC items: vacuum pumps, hydraulic pumps (making water to circulate in magnets and power converters) - Power consumption of the total number of pumps, assuming TMP in a good vacuum regime (0,5 kW each? Or less?)

### 3.3.3 Sum of the consumption from all components

The contribution of the chillers was included in the calculation, by adding a 33% (COP = 3) to the overall total.

Summing up all the above mentioned contributions an overall average power consumption of ~ 260 kW is calculated, which is broken down into its major contributions in table 5.

|                                 |                |
|---------------------------------|----------------|
| Synch + extraction lines        | 130,647.5      |
| Particle dependent LEBT         | 5,400          |
| Common LEBT + MEBT              | 16,744.5       |
| <b>LINAC</b>                    | <b>41,876</b>  |
| <b>Total</b>                    | <b>194,668</b> |
| <b>Total including chillers</b> | <b>258,908</b> |

Table 5 – Sum of all major power consumption contributions of the CNAO facility, including 33% due to the chillers for cooling water treatments.

### 3.4 Power consumption in therapy and non-therapy hours.

For the sake of completeness, and in view of a facility – like the SEEIST one – which is to be used 50% for therapy and 50% for research, it is useful to consider that the typical conditions



of use of CNAO for the two purposes is different and to separate the average power consumption for therapy and for research.

Typically, medical physicists work 8 hours/day on Saturdays and Sundays for therapy setup. For an additional equivalent time, machine physicists perform routine tests, QA tests, developments (e.g. RF knockout) and external groups perform physics tests. The total fraction of use is hence of around 16/24 hours during weekend days and from 22pm to 6 am from Monday to Friday.

Table 6 show the splitting of “equivalent” beam days, during 2020, for the two scopes. The non-therapy use, even in a therapy-oriented machine like CNAO, amounts to nearly 30%.

| Month          | Equivalent beam days | Equivalent clinical beam days | %             |
|----------------|----------------------|-------------------------------|---------------|
| January        | 6.69                 | 4.53                          | 67.74%        |
| February       | 7.73                 | 5.26                          | 68.01%        |
| March          | 7.97                 | 5.95                          | 74.63%        |
| April          | 7.52                 | 5.52                          | 73.32%        |
| May            | 7.31                 | 5.30                          | 72.51%        |
| June           | 8.34                 | 5.71                          | 68.49%        |
| July           | 7.67                 | 5.20                          | 67.83%        |
| August         | 6.72                 | 4.85                          | 72.18%        |
| September      | 6.39                 | 4.93                          | 77.17%        |
| October        | 6.96                 | 5.05                          | 72.59%        |
| November       | 8.21                 | 5.79                          | 70.53%        |
| December       | 7.53                 | 5.21                          | 69.19%        |
| <b>Average</b> | <b>7.42</b>          | <b>5.27</b>                   | <b>71.09%</b> |

Table 6 – Monthly equivalent beam days (i.e. on-time) of the facility in 2020 and, aside, the fraction and the percentage of such days that have been used for therapy.

The power consumption in non-therapy hours is worth being calculated since, as shown in fig.8 with a sample day, it is occasionally much more expensive.

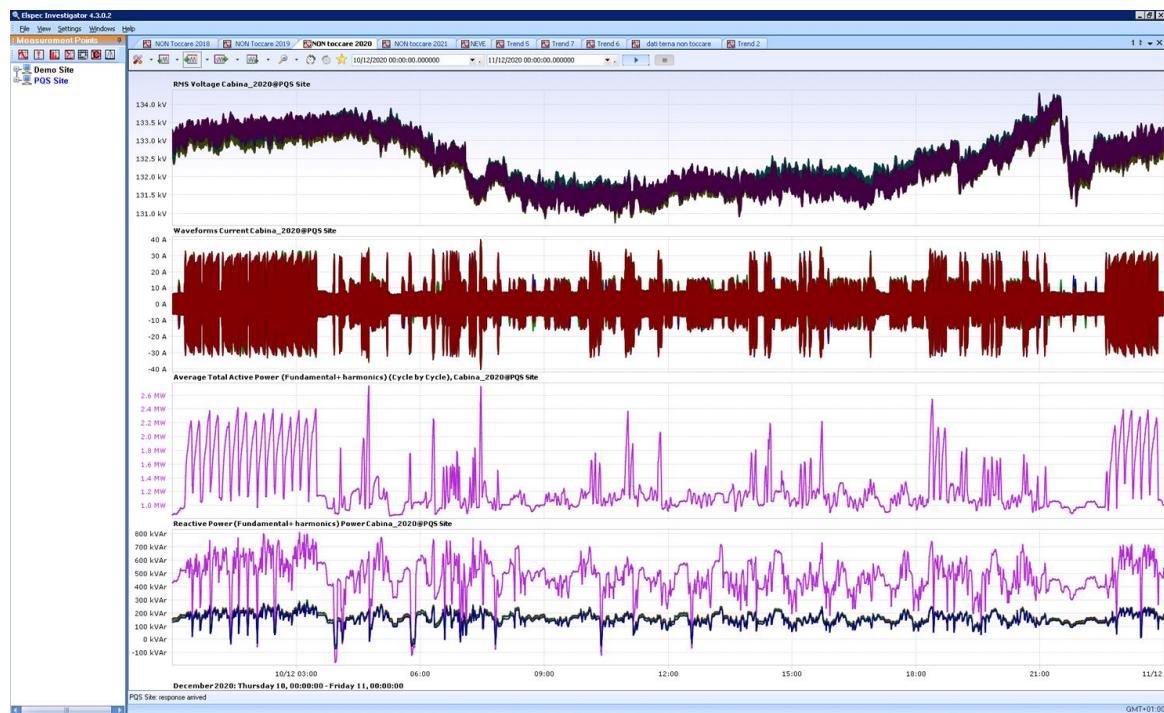


Fig.8 – On Dec 10, 2020, the average power during therapy hours was 95 kW and during non-therapy hours 518 kW.

### 3.4.1 Distribution of energies for 2020

#### To be written

*(From the CNAO log file, with cycle duration and respective diplo current values, a histogram on the distribution of accelerated beam energy can be derived, split into energies for p and for C beams. Two histograms are of interest: the one for therapy hours (6 am to 10 pm on working days) and the one for therapy research, accelerator tests and physics runs (in the remaining time).*

*Histograms...)*

### 3.4.2 Use of the various beam lines

#### To be written

*(The CNAO log files gives information on the fraction of time for which the vertical beam line is used, versus the horizontal ones.*

*Data...)*

It may be noted, incidentally, that the peak power consumption of the facility, during magnet ramps, may achieve a maximum of around 7 MW.

## 4 Layout options for the NIMMS/SEEIST facility with room temperature and with superconducting magnet.

### Introduction, to be written

- *(What is in common in all layouts, with the SEEIST initial layout as reference*
- *The same linac as in HIT/CNAO until further developments;*
- *The HEBT lines differ only in the initial part, depending on which of the 4 layouts;*
- *gantry (speculative, if it were NC); data on the NC gantry consumption from HIT?*
- *For each of the considered cases, reasonable limits of maximum/minimum power consumptions should be given.)*

### 4.1 NC cases.

#### A. The PIMMS-line design

*From EB design, broken down list of the relevant components, ref. to the file, conclusions on the consumptions. Synchrotron, beam lines.*

#### B. The DBA design

*From the EB design, broken down list of the relevant components, ref. to the file, conclusions on the consumptions. Synchrotron, beam lines.*

#### C. A room-T gantry

*Ref. from HIT (if any)*

## 4.2 Use of ramped SC magnets for the NIMMS/SEEIST facility.

As stated above, to develop NIMMS/SEEIST layouts making use of superconducting magnets (SC dipoles in particular) would allow to build a hadrontherapy synchrotron and gantry with a significantly smaller footprint. The SC option has been already realized at HIMAC (NIRS-Chiba, J) for a 360° SC gantry, the size of which is much smaller than the corresponding room T version of HIT (DFFZ, Heidelberg, D). Thanks to the progress in the SC magnets field, and perhaps limiting the rotation to 180°, the size, weight, footprint and cost of future gantries can be further reduced. SC magnets can be considered, in principle, also for the synchrotron. For He cooling, either cryocoolers or a refrigerator can be considered. Cryocoolers are simpler to handle in a hospital environment, as they are modular and their swift replacement does not require high cryogenics qualifications. Refrigerator, requiring proper maintenance and assistance contracts, are – on the other hand - a topologically simpler and less power demanding solution. In case a refrigerator was chosen, one could extend the SC option to dipoles of the HEBT lines and to quadrupoles of synchrotron and beam lines, if convenient.

It remains to be assessed, whether a hadrontherapy facility based on SC magnets consumes less electrical energy and required less installed power than one based on room temperature ones. One has hence to compare the power dissipated during the operational time of the facility in the two cases, taking into account that a cryogenic facility remains on – with a good fraction of the power consumption related to the static losses of the cold masses – even when the machine is an idle state.

Besides power consumption, finally, capital investment in magnets and power converters, powering and cooling facilities, electrical infrastructures themselves must be compared in order to choose the most convenient solution.

Let us assess the comparison of electrical power consumptions, in a first instance.

For fast pulsed dipoles it is particularly critical to evaluate and control the power dissipated in the cold mass during the rapid cycle of the magnet, which adds up to the static losses

The main dissipative sources are:

- magnetic hysteresis in the superconductor
- eddy currents in the conductor (inter-filament and inter-strand coupling currents) and other coil components.
- eddy currents in other magnet components, namely collar, beam pipe and yoke (or coil former in case a CCT would be used),
- magnetic hysteresis of the iron yoke.

## 4.3 SC Gantry

### 4.3.1 Mikko Karppinen

The layout of the SIGRUM SC gantry is shown in fig. 9, featuring 5 SC combined function dipoles (at 3 T dipole field and 2 T/m quadrupole component gradient) and 3 SC quadrupoles (40 T/m). 7 room-T quadrupoles (25 T/m) complete the main magnet configuration. The increase rate of the dipole field is 0,1 T/s.

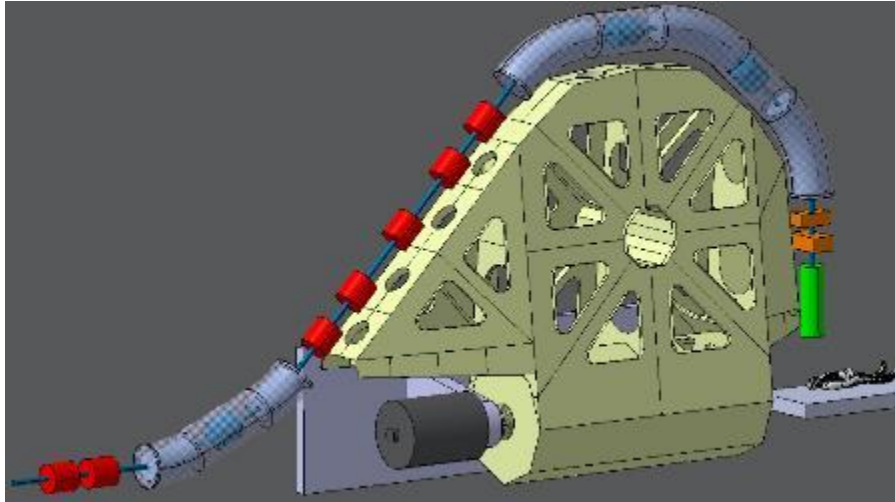


Fig. 9 - 3D image of the TERA/NIMMS SC gantry. It is 16 m long for a total weight of less than 30 tons (for the rotating part)

#### 4.3.2 SC magnets

Details on the combined functions dipoles are given in fig. 10, and the associated field intensity is shown in the aside plots.

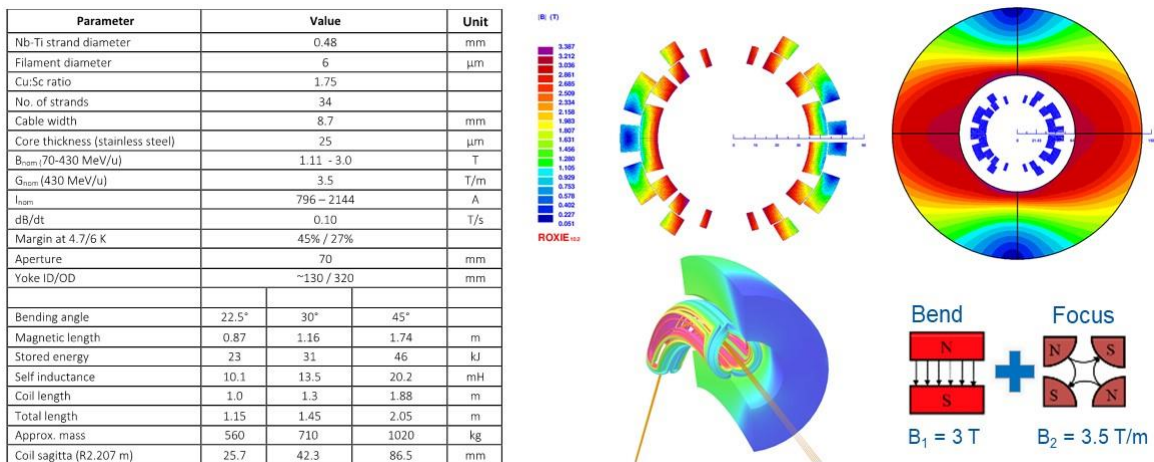


Fig.10 - Dataset and field distribution of the combined-function dipoles of the SC gantry

The mechanical concept is described in Ref. [\*]. A delicate point is the estimation of the transient losses, understand the T-gradient between the coils and the thermalisation point, to verify the operational margins and to estimate the required cooling power. Transient losses are due to the composition of inter-filament coupling losses, inter-strand coupling losses, eddy currents in the wedges, persistent losses (...).

The transient analysis assumes subsequent field ramps from 0 to 2144 A and back to 0 in periods of 60 s (fig. 11). As a thermal reference, two perfect heat sinks at 4.5K in the iron yoke are considered.

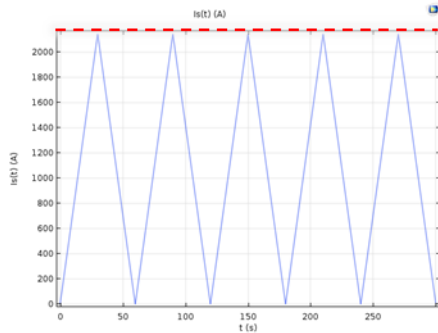


Fig. 11 - Transient behaviour of the combined function magnets of the SC gantry

It is shown, from the simulations, that in these conditions a quasi steady state condition at  $T_{max}=4,69K$  is achieved after 60 s. It should be noted that this cycle is a pessimistic since, in the real case, the magnet current would increase with plateaus of a few seconds each, allowing a slightly easier thermalization.

**Scaling this case from the experimental conditions of the Discorap experiment, one obtains a total coil loss of 1,25 W/m, which sum up with ~ 0,5 W/m loss for eddy currents in collars, collaring keys and iron. The total sum is lower than 2 W/m.**

**Total length of dipoles: ~ 7 m,  $2 \times 0,87 = 1,74$  m ( $22,5^\circ$ );  $3 \times 1,74 = 5,22$  m ( $45^\circ$ ). For 2 W/m, the overall transient losses of the combined-function dipoles can be estimated to be  $P_{tot,dip}=14$  W.**

Is this all for the dipoles, except the static losses?

Why is the power dissipation of the SC quads not given?

#### 4.3.3 Rob van Weelderren

Overall losses of dipoles and quadrupoles, including dynamic losses, static losses and currents leads appear to be, excluding powering:

From the table of slide 2

- for each  $45^\circ$  dipole 1,55 W
- for each  $22,5^\circ$  dipole 1,55 W
- for each quadrupole 1,55 W
- for the cold-warm transition (of each, I assume) 0,5 W

In total  $P_{SC-magnets} = 8 \times (1,55 + 0,5) W = 16,4 W$

From the text above the table, in the same slide:  $9,4 + 2,9 + CL$ , i.e.  $P_{SC-magnets} = 12,3 W + CLs$

Current leads.

The power consumption of the CLs differs for vapour cooled (1 W/kA) and for HTS-vapour cooled ( $\ll 1$  W/kA) solutions. The power consumption would be 15 W in the first case (a high value, which – added to the power consumption of the magnets – dictates the use of a liquefier), and marginal in the second case, in which dedicated cryocoolers for the CLs could be used.

Cryogenic equipment

For the dynamic and static losses (12-13 W) of all the gantry one can use:

- 7x2 stage cryocoolers,

or

- a small refrigerator for 5K supercritical He.

For the CLs, one can use: in case of HTS leads, suitable cryocoolers; for any other lead type, a small scale refrigerator.

Two types of cryocoolers are proposed, with the compressor unit (requiring water cooling and 3-phase power supply) at ground and the cryocooler heads rotating with the gantry. They feature a cooling power of 1,8-2 W each. A total number of 8 cryocoolers is needed, plus 2 for contingency, not including the CLs (in the assumption that they are HTS-vapour cooled with negligible consumption). Each of them consumes 7 kW, for an overall power consumption of 56-kW.

4.3.4 Cost of the cryogenic equipment: a comparison

Cost exercise on the plants (both cold and warm parts). Is the following exercise “official”?

As to the cryo-cooler cost, the following formula applies:  $Cost = 37 * P^{0.38}$  (k\$), with P being the cooling power at 4,5K. For 16 W, Cost=106k\$.

If the refrigerator for 5K supercritical He is used,  $Cost = 2600 * (P/1000)^{0.63}$  (k\$) with P being the refrigeration produced in kW at 4,5K. What is the plug power of the refrigerator, for 16 W at 4,5K? For 16 W, Cost=\*\*\* k\$.

For the particular case of the SC gantry, the use of the refrigerator is justified if it is used for other parts of the facility.

4.3.5 Remaining questions.

- Standard field ramp rate: 0,1 T/s is OK? EB
- Which specs for the SC magnets power supplies?

4.3.6 NC magnets

To be written

(Synchrotron remaining room-T components and their consumption. Estimated number of quadrupoles: 6. With EB and MS estimate the required gradient vs. beam energy and their total power consumption.)

4.4 SC synchrotron versions.

4.4.1 SC magnets

The power dissipation of the NIMMS/SEEIST synchrotron dipoles is estimated with reference to the closest example of a SC magnet of similar characteristics, which is the one developed by INFN in cofounding with GSI in the framework of the DISCORAP project [REF], related to the FAIR SIS300 machine project.

The main specifications of the DISCORAP dipole are shown in table 7.

|                   |               |
|-------------------|---------------|
| Nominal field     | 1.5 T – 4.5 T |
| Nominal ramp rate | 1 T/s         |

|  |                   |
|--|-------------------|
| Maximum current                          | <b>8926 A</b>     |
| Nominal current rate                     | <b>1983 A/s</b>   |
| Cable critical current @ T=4.2 K & B=5 T | 18540 A           |
| Voltage during ramp rate                 | <b>23 V</b>       |
| Maximum magnetic energy                  | 459 kJ            |
| Coil aperture diameter                   | 100 mm            |
| Magnetic length                          | 3.878 m           |
| Curvature radius                         | 66.667 m          |
| Bending angle                            | 6 2/3 deg         |
| Yoke inner / outer radius @ 300 K        | 96.85 mm / 240 mm |
| Reference radius for field quality       | 35 mm             |

Table 7 - Specifications list of the DISCORAP dipole magnet

Table 8 summarizes the losses calculated, for a ramp rate of 1 T/s, for the DISCORAP magnet.

| Bo           | In straight section (W/m) |              |              | In each coil end (W) |             |             | % in 3.9 m long magnet |             |             |
|--------------|---------------------------|--------------|--------------|----------------------|-------------|-------------|------------------------|-------------|-------------|
|              | 1.5 T                     | 3.0 T        | 4.5 T        | 1.5 T                | 3.0 T       | 4.5 T       | 1.5 T                  | 3.0 T       | 4.5 T       |
| Conductor    | <b>4.500</b>              | <b>3.300</b> | <b>2.600</b> | 0.630                | 0.462       | 0.364       | 51%                    | 38%         | 36%         |
| Collar eddy  | 0.006                     | 0.006        | 0.006        | 0.144                | 0.393       | 0.197       | 1%                     | 2%          | 1%          |
| Yoke eddy    | 0.002                     | 0.002        | 0.002        | 0.234                | 1.111       | 0.978       | 1%                     | 6%          | 7%          |
| Collar pins  | 0.140                     | 0.138        | 0.102        | 0.004                | 0.004       | 0.004       | 1%                     | 2%          | 1%          |
| Collar keys  | 0.568                     | 0.552        | 0.436        | 0.013                | 0.014       | 0.014       | 6%                     | 6%          | 6%          |
| Yoke pins    | 0.062                     | <b>0.533</b> | <b>0.167</b> | 0.030                | 0.035       | 0.049       | 1%                     | 6%          | 2%          |
| Yoke keys    | 0.000                     | 0.000        | 0.000        | 0.058                | 0.169       | 0.074       | 0%                     | 1%          | 1%          |
| Yoke hyst.   | <b>1.800</b>              | <b>1.800</b> | <b>1.800</b> | 0.351                | 0.351       | 0.351       | 21%                    | 21%         | 25%         |
| Coil protec. | 0.484                     | 0.484        | 0.484        | 0.094                | 0.094       | 0.094       | 6%                     | 6%          | 7%          |
| Beam tube    | <b>1.000</b>              | <b>1.000</b> | <b>1.000</b> | 0.195                | 0.195       | 0.195       | 12%                    | 12%         | 14%         |
| <b>TOTAL</b> | <b>8.56</b>               | <b>7.82</b>  | <b>6.60</b>  | <b>1.75</b>          | <b>2.83</b> | <b>2.32</b> | <b>100%</b>            | <b>100%</b> | <b>100%</b> |

Table 8 - Calculated contribution of various sources of losses for the DISCORAP dipole magnet.

During the tests, performed in liquid helium (while the magnet has been designed to operate in supercritical He), the field was ramped up and down at varying values of  $\delta B/\delta t$ , as shown in fig. 12, although with a duty cycle which is smaller than the one required from hadrontherapy machines (the latter featuring an interval of ~ **0,5 s between consecutive cycles**).

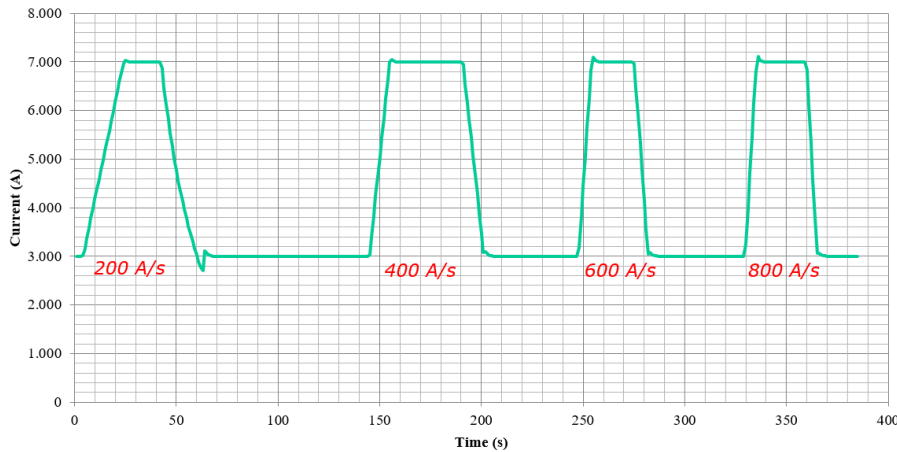


Fig. 12 - experimental cycles of the DISCORAP magnet, at various ramp rates **GB: but they are far slower than in the specs (Table 7), i.e. 2000 A/s**

The experiments with this single prototype magnet was faced with quench limitations, which did not allow to exceed a ramp rate of 0,7 T/s. In addition, the measured losses were smaller than the computed ones, as shown in fig. 13.

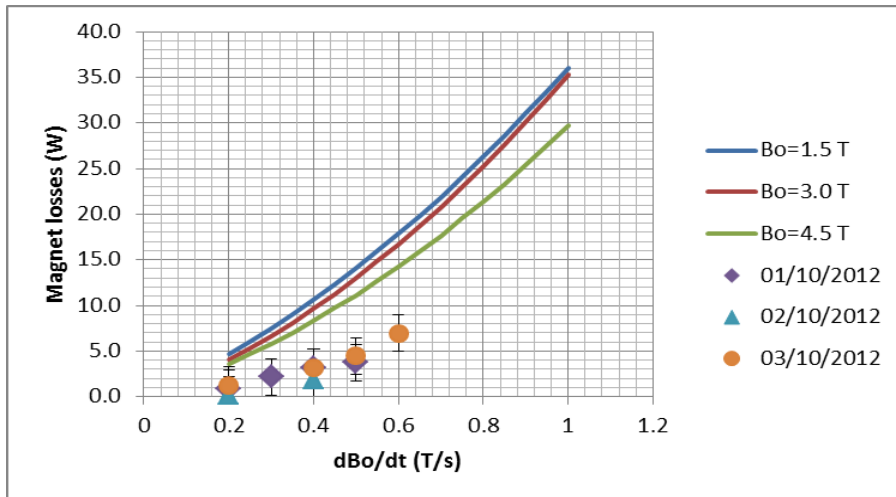


Fig.13 - Computed (at various final field levels) and measured losses on the DISCORAP magnet.

We propose to consider the computed losses **for 3.0 T** as a realistic/pessimistic indication for the losses of the NIMMS/SEEIST synchrotron. A value of **30 W at 1 T/s** can be taken. Considering that the DISCORAP magnet is 3.8 m long, **a total power dissipation of around 8 W/m can be considered as a reference for NIMMS/SEEIST.**

**Can we provisionally trust fig. 13, for the higher rates? And ... why do the losses increase with decreasing final field? Scaling of the losses with the field is needed, for comparison with the NC solutions (=the typical therapy cycle beam energy will be assumed, not the maximum one).**

#### 4.4.2 Additional open points for GB.

**For gantry AND for synchrotron magnets, define the energy consumption as the sum of several contributions:**

- static consumption (B=0);

- consumption when the power supplies are idle (nothing more on the magnets, some electrical consumption at the power converter plug)
- consumption during a ramp (and low consumption vs. ramp rate)
- consumption at the flattop (if any)

Indeed, similarly to the NC magnets The typical (=average power) cycle must be considered

What is the weight of the repetition rate of the cycle? At CNAO the pause between the end of a ramp-down and start of the next ramp-up is around 1 s. Can we afford a longer interval? EB... Would it help the thermal stabilization and lower power consumption?

Which is the cryogenics inertia towards short consumptions, which do not raise the temperature beyond  $T_C$ ?

Translation from magnet losses (of various types) and power at the cryogenic plug: which rules, for the cryogenic "plant" chosen?

#### 4.4.3 NC magnets

Synchrotron remaining room-T components and their consumption.

#### 4.4.4 Square-shaped

To be written

#### 4.4.5 Triangle-shaped

To be written

## 5 Method adopted to estimate power consumption at the NIMMS/SEEIST synchrotron-based facility

### 5.1.1 Universal model for the energy efficiency comparison

To be written

- Introduction, build-up of a universal comparison worksheet.
- For the moment being, the HIT/CNAO linac is assumed for all
- Propose and agree upon an official splitting between the two.

### 5.1.2 Energy use for therapy treatment

To be written

(Histogram at CNAO used for reference, for therapy hours.)

### 5.1.3 Energy use for therapy tests, machine tests, basic science

To be written

(Use average power consumption at CNAO for the mixed developments as a first reference, to be discussed and agreed upon: for R&D the machine is often used at the maximum energy, and with no interruptions (like those dictated by patient needs)

## 5.2 Cryogenic efficiency

To be written

*(Worst/best scenarios to be considered.*

*Estimate cryogenic efficiencies “at the plug” for the power consumption of SC magnets for both gantry and synchrotron. Split the considerations for the various cryogenics options:*

- *Cryocoolers on gantry*
- *Cryocoolers on gantry with compressors on ground*
- *Cryocoolers for synchrotron and beamline*
- *Liquifier for synchrotron and beam lines)*

## 5.3 Overall power consumption of the two SC versions

*(with the above consumption input and statistics on use of the facility from previous chapter)*

Rob: 80-110 kW is the estimated power consumption of the gantry for the cold mass only.

## 6 Ancillary topics to be addressed.

To be written

Technical specifications, capital and maintenance cost of the technical infrastructures in the room-T and SC cases.

Multi-E extraction: assessment in the two cases, if applicable to both



| Riferimento                    | DocID          | Rev. | Validità   |
|--------------------------------|----------------|------|------------|
| Energy Efficiency NIMMS/SEEIST | NIMMS-NOTE-xxx | 0.1  | 2021-02-09 |

## 7 Added notes, for further possible considerations

### 7.1 LNL Infrastructure from high to medium voltage lines

Cavo interrato da 132 kV, per Pmax di 120 MW (come cavo).. La sottostazione ha due stadi di trasformatori 132/20 kV di cui uno da circa 30 MW installato (35 MW con ventilazione) e la predisposizione per un secondo.

TUTTO è costato 6 M€, valore 2006. Circa 50-50 tra cavo interrato e tutto il resto.

La potenza "installata" a LNL è di 15 MW, con un coefficiente medio di utilizzo (contemporaneo) del 30%, cioè 4 MW, quando c'è tutto che va.

La bolletta elettrica è di 2,7 M€/anno (quando si è a regime), mentre è di 1,6 M€ senza attività ad acceleratori ed esperimenti.

Il ciclotrone da solo consuma solo 100 kW, tutto il suo edificio 1 MW.

I cavi di arrivo sono stati interrati anche come condizione alla loro installazione (permesso), sono isolati in SF6 (cosiddetta "esecuzione blindata").

In tal modo il real estate passa da 150x150 m (LNF) a 30x15 m (LNL).

Essendo sfasati tra loro non irradiano (il B si compensa nella regione tra loro, ... sarà vero? Gb).

Il cavo dalla sottostazione di Camin a LNL è di circa 3,5 km.

Ogni 2 anni ENEL ne chiede la sospensione del servizio per 1 settimana per manutenzioni nella cabina a monte.

In quei casi la vecchia cabina di consegna da 20 kV alimenta i LNL fino ad un max di 20 MW di potenza (viene dalla Z.I. di LNL).

Sulla linea da 132 kV siamo "in antenna, cioè la linea si chiude sull'installazione di LNL. La 20 kV invece è collegata da un lato alla Z.I. di Camin dall'altro ad Agripolis.

Se fuori terra sarebbe stata più fangile e più soggetta a manutenzioni, scarica più facilmente, fulmini ecc.

Con l'occasione dei lavori si è sostituito un cavo in aria con uno interrato anche dalla cabina di consegna a 20 kV fino a TAP.

Costi di manutenzione: ragionevoli 30 k€/anno: verifiche interruttori, olio per la parte meccanica, ecc. gestito da ENEL.

La sottostazione dovrebbe essere presidiata, anche da remoto, per avvisare di scariche ecc., in pratica non lo è.

Sulla linea tra sottostazione e cabina di consegna c'è la piastra (futura centrale tecnologica per altre installazioni, da cui parte un cavo sotterraneo che alimenta direttamente l'edificio ciclotrone.

Prezzo tasse incluse energia elettrica oggi: circa 18 c€/kWh (5-7 di cui sono costo dell'energia).

### 7.2 CNAO maximum peak power needed, infrastructure details and electrical contract

Occasionally up to 7 MW of power has been achieved (approximately, 5 for the dipoles, 2 MW for the 90° dipole, 0,5 MW for the septa, the rest for quadrupoles, sextupoles, etc.) for



|   |                         |             |                        |
|---|-------------------------|-------------|------------------------|
| Riferimento<br>Energy Efficiency NIMMS/SEEIST | DocID<br>NIMMS-NOTE-xxx | Rev.<br>0.1 | Validità<br>2021-02-09 |
|---|-------------------------|-------------|------------------------|

very short time fractions. The 90° vertical dipole, for the very unfrequent occasions in which it works at full power, can achieve a peak power consumption of 5 MW.

According to the electrical contract, a maximum 16 MW peak power is foreseen. Transformers, cables and related components are sized for 20 MVA (and 25 kW are spent for steady losses in transformers).

The HV beam line (132 kV) and substation requires maintenance on transformers and other components. Equivalent maintenance on a medium-voltage line (or two, for useful redundancy) would be by far less expensive.

**The cost of an electrical infrastructure, as a function of the installed power, should be calculated.**

### **7.3 Cost of energy**

At CNAO and INFN, all taxes included, the cost of electricity is 0,18-0,20 €/kwh, despite the rather different installations, average and peak power values required.

### **7.4 Options for layout improvement, impacting on overall efficiency**

Location of the operation console, vs. the power converters hall.

Distance from power converters hall and machine (in CNAO, given the distance, purchase of larger cables is considered, the cost of which would be amortized by lower warmup and related power consumption in the long run.